Line detection in images showing significant lens distortion and application to distortion correction

M. Alemán-Flores[a], L. Alvarez[a], L. Gomez[b], D. Santana-Cedrés[a,*]

[a] *CTIM: Centro de I+D de Tecnologías de la Imagen. Departamento de Informática y Sistemas. Universidad de Las Palmas de Gran Canaria. Campus de Tafira, 35017, Las Palmas. Spain.*

[b] *CTIM: Centro de I+D de Tecnologías de la Imagen. Departamento de Ingeniería Electrónica y Automática. Universidad de Las Palmas de Gran Canaria. Campus de Tafira, 35017, Las Palmas. Spain.*

Abstract

Lines are one of the basic primitives used by the perceptual system to analyze and interpret a scene. Therefore, line detection is a very important issue for the robustness and flexibility of Computer Vision systems. However, in the case of images showing a significant lens distortion, standard line detection methods fail because lines are not straight. In this paper we present a new technique to deal with this problem: we propose to extend the usual Hough representation by introducing a new parameter which corresponds to the lens distortion, in such a way that the search space is a three-dimensional space, which includes orientation, distance to the origin and also distortion. Using the collection of distorted lines which have been recovered, we are able to estimate the lens distortion, remove it and create a new distortion-free image by using a two-parameter lens distortion model. We present some

*Corresponding author: Tel. +34 928 458708

Email addresses: maleman@ctim.es (M. Alemán-Flores), lalvarez@ctim.es (L. Alvarez), lgomez@ctim.es (L. Gomez), dsantana@ctim.es (D. Santana-Cedrés)

Preprint submitted to Pattern Recognition Letters *May 7, 2013*

experiments in a variety of images which show the ability of the proposed approach to extract lines in images showing a significant lens distortion.
Keywords: Line detection, lens distortion, Hough transform.

1. Introduction

Most Computer Vision algorithms usually rely on the well-known pinhole camera model (see for instance Faugeras (1993), Faugeras et al. (2001) or Tsai (1987)). This linear model assumes that the projection of 3D lines onto the camera plane are 2D lines. However, wide-angle lenses, especially most commercially available low-cost cameras, introduce a severe optical distortion that must be corrected to account for the foundations of the 3D to 2D projection.

The distortion is mainly due to the imperfection of the lens and the misalignment of the optical system. Among all possible distortions, lens radial distortion is considered the most important for low-cost cameras. It causes barrel distortion at short focal lengths as well as pincushion distortion at longer focal lengths.

The basic standard model for barrel and pincushion distortion correction (see for instance Brown (1971), Hartley and Zisserman (2004) or McGlone (1980)) is the simple radial distortion model given by the expression

$$\begin{pmatrix} \hat{x} - x_c \\ \hat{y} - y_c \end{pmatrix} = L(r) \begin{pmatrix} x - x_c \\ y - y_c \end{pmatrix}, \tag{1}$$

where (x, y) is the original (distorted) point, $(\hat{x}, \hat{y})$ is the corrected (undistorted) point, (x_c, y_c) is the center of the camera distortion model (the center of the image), $r=\sqrt{(x-x_c)^2+(y-y_c)^2}$ and $L(r)$ is the function which defines the shape of the distortion model. $L(r)$ can be approximated by a Taylor expansion as follows:

$$L(r) = k_0 + k_1 r^2 + k_2 r^4 + ..., \tag{2}$$

where the set $\mathbf{k} = (k_0, k_1, ..., k_{N_k})^T$ consists of the distortion parameters which must be estimated from image measurements, usually by means of nonlinear optimization techniques by imposing the requirement that 3D lines in the image must be projected onto 2D straight lines.

Two alternatives are possible to identify and select the visible straight lines in the scene: one (standard or *classical*) which uses human intervention (Alvarez et al., 2008; Brown, 1971; Devernay and Faugeras, 2001) and a more recent approach that identifies a minimum set of straight lines with no human intervention (Bukhari and Dailey, 2012). The classical approach, although more robust than the unsupervised techniques, becomes slow and inefficient when processing large sets of images, where an automatic method seems more adequate.

The objective of this work is twofold. On the one hand, we propose a new unsupervised approach to detect lines in images showing a significant lens radial distortion. The identification of those lines is performed through a three-dimensional Hough space which includes the radial distortion as a parameter. This approach is new in the sense that the lens distortion is embedded into the Hough space and, in this manner, a better estimation of actual straight lines is obtained. On the other hand, provided the existing straight lines, we obtain the corresponding distortion-free image.

The organization of this paper is as follows: Section 2 summarizes the state of the art of radial distortion models, describing those requiring human intervention as well as the most recent approaches. Section 3 presents our adaptation of the Hough transform to detect the lines in the scene when the image shows a strong distortion. Section 4 deals with the application of the proposed method to a relevant problem in Computer Vision: the correction of lens distortion in images showing radial distortion. Section 5 explains the experimental setup and the evaluation of the proposal on several images showing significant radial distortion. Finally, some conclusions are drawn.

2. Related work

This section deals with some of the relevant literature regarding the radial distortion. Then, a revision of how these methods are applied to images is presented.

During the last decades, several methods for removing the radial distortion from images have been extensively researched. There exist mainly two widely accepted lens distortion models: the polynomial model and the division model.

The polynomial model (see equation (2)), has been widely applied because it provides an excellent trade-off between complexity and accuracy. The most applied polynomial model is the even-order polynomial model, which is coherent with the fact that the even distortion parameters are more relevant than the odd ones (see for instance Brown (1971)).

The complexity of the polynomial model is given by the number of terms of the Taylor expansion used to approximate $L(r)$. Some authors use a single parameter model (Devernay and Faugeras, 2001), (Wang et al., 2009) which, as shown in (Strand and Hayman, 2005), provides similar results as the division model for the case of also using a single distortion parameter.

The one-parameter model, as (Devernay and Faugeras, 2001) reports, achieves an accuracy of about 0.1 pixels in image space using lenses exhibiting large distortion, when used for camera calibration (Faugeras and Toscani, 1987). However, (Devernay and Faugeras, 2001) also reports that for cases of significant radial distortion, such as fish-eye lenses or higher distortion lenses, the one-parameter model is not recommended.

The two-parameter model is the usual approach in some related works (see for instance Kang (2000), or Alvarez et al. (2008)) because it is simple, accurate, and can be estimated using just image information (known lines in the scene provide enough information for simple cases). In particular, Alvarez, Gomez and Sendra (Alvarez et al., 2008) proposed an algebraic method to compute lens distortion models by correcting the line distortion induced by the lens distortion. This algebraic model is suitable for correcting significant radial distortion and is also highly efficient in terms of computational cost. An on-line demo of the implementation of this algebraic method can be found in (Alvarez et al., 2010).

Other more complex two-parameter radial distortion models include depth field estimation (Alvarez et al., 2011; Bräuer-Burchardt et al., 2006; Fraser and Shortis, 1992) or zoom effects (Alvarez et al., 2012).

Once a lens distortion model has been selected, we must decide how to apply it. Plumb-line methods (Alvarez et al., 2008, 2011; Brown, 1971; Devernay and Faugeras, 2001; Wang et al., 2009) rely on the human-supervised identification of some known straight lines in one or more images (a user identifies the lines and *manually* marks some points on the distorted lines).

As a consequence of the human intervention, these methods are robust, independent of the camera parameters, and do not need any calibration pattern (see Zhang (2000) for a point correspondence method) or images acquired under a particular camera motion (see for instance, Faugeras et al. (1992) or Ramalingam et al. (2010)). However, these methods are slow and tedious for the case of dealing with large sets of images. From the set of selected lines, a nonlinear optimization problem is stated in terms of minimizing the mean square error between the observed and the predicted image points.

Recently, some new approaches not relying on user intervention have emerged. In (Gonzalez-Aguilera et al., 2011), Canny edge detector and Burns segmentation algorithm are used to automatically extract the set of lines from a single image. In addition, it is required to identify at least a vanishing point, which is done by using the Gaussian sphere method (Barnard, 1983).

In (Bukhari and Dailey, 2010) and (Bukhari and Dailey, 2012), an automatic method to correct lens radial distortion is discussed. This method works on a single image and no human intervention or special calibration pattern are required. The method applies Fitzgibbon's division model (Fitzgibbon, 2001) using a single distortion parameter to estimate the distortion from a set of automatically detected non-overlapping circular arcs. Afterwards, a nonlinear optimization is carried out to improve the estimation of the distortion parameter in the sense of least squares metric.

The proposal in (Bukhari and Dailey, 2012) works well for a wide number of images showing radial distortion, but, for some cases, it is unable to efficiently correct the distortion due to some problems related to the extraction of the straight lines within the image (it is not able to identify very long lines, but a piecewise version of them).

In the next section, the method we used to extract the lines is detailed. As main differences with (Bukhari and Dailey, 2012), we consider only the longest lines within the image (instead of circular arcs) and a fast algebraic two-parameter lens distortion model is applied (in (Bukhari and Dailey, 2012), Fitzgibbon's one-parameter model is used).

3. A new Hough space including a lens distortion parameter

The Hough transform is a widely used technique in image processing which allows extracting the relevant shapes in an image. The shapes which are searched for must be expressed in a parametric form, and therefore, it is mainly used for the detection of geometric shapes such as lines, circles or ellipses. It was originally conceived to identify lines (Hough, 1959), but the generalized Hough transform was later introduced to deal with more complex shapes (Duda and Hart, 1972; Ballard, 1981).

In order to find imperfect instances of the required shape, the Hough transform uses a voting procedure within a parameter space. This translates into an array where the votes are accumulated. Finally, the local maxima within this array provide the most reliable instances of the shape. One of the main advantages of the Hough transform is the fact that it is not affected by gaps in the contours of the shapes. However, one of its main drawbacks is the computational cost, which mainly depends on the number of parameters, i.e. the degrees of freedom of the shape, and the number of values they can take.

The problem of extracting straight lines from a single image has been extensively researched (Chung and Lin, 2010; Guru et al., 2004; Lee et al., 2006). However, in our particular case, we try to extract lines in images suffering from a significant distortion, which stands as a complex pattern recognition problem. If distortion is not taken into account, the classical Hough transform fails, since the points belonging to the same line do not vote for the same set of parameters, thus being considered as segments of different lines. For this reason, a distortion parameter should be included in the Hough space. Hence, a line in our space is described by three parameters: distance to the origin, orientation and distortion.

For carrying out our voting procedure, we first extract the edge points in the image and estimate the magnitude and orientation of the edge. Those points where the magnitude is significant vote for a set of lines in our Hough space. In particular, for every value of the distortion parameter, we determine the lines whose orientation differs less than a certain threshold from the orientation of the edge and are close enough to the point. In order to give a higher weight to the closer points, the vote v, which is added to the corresponding line, is calculated as

$$v = 1/(1 + d), \tag{3}$$

where d is the distance from the point to the line.

We can assume that the distortion which affects all lines within an image is the same for all of them. This means that a single value for the distortion parameter is estimated for the whole image. We remark that, at this stage, a lens distortion with a single parameter is used. Furthermore, the longer the lines, the more reliable the information they provide. For these reasons, those lines which are too short are directly rejected, and we then select only the n longest lines for each possible value of the distortion parameter. The actual value will make the edge points fit into the line equations, instead of randomly voting for arbitrary lines.

Once the n longest lines have been selected for every value of the distortion parameter, we must estimate which is the right one. We calculate a measure for the reliability of each value of the distortion parameter which favors those lines with a higher score and, therefore, the values for which the longest lines have been detected. The reliability measure r_i for the i^{th} value is

$$r_i = \sum_{j=1}^{n} (s_j^i)^{\frac{3}{2}}, \tag{4}$$

where s_j^i is the total score of the j^{th} line of the i^{th} value. Since $x \to x^{\frac{3}{2}}$ is a convex function, those sets which contain the longest lines will receive a higher score.

We use a single parameter distortion model based on the following function:

$$L(r) = 1 + k_1 r^2, \tag{5}$$

where k_1 is the distortion parameter. When the lens distortion is corrected, the distance r from a point to the center of distortion is modified in the following way:

$$\hat{r} = (1 + k_1 r^2) r. \tag{6}$$

In particular, if we note by r_{max} the distance from center of distortion to the furthest point in the image, and we express the variation of r_{max} in terms of a percentage p, we obtain that

$$p = \frac{\hat{r}_{max} - r_{max}}{r_{max}} = \frac{(1 + k_1 r_{max}^2) r_{max} - r_{max}}{r_{max}} = k_1 r_{max}^2, \tag{7}$$

and, therefore, according to the percentage p, we can write k_1 as

$$k_1 = \frac{p}{r_{max}^2}. \tag{8}$$

Instead of directly using the value of k_1 in the Hough space, we work with the normalized parameter p. One important advantage of taking the percentage p as the distortion parameter in the Hough space is that this parameter is normalized in terms of distortion correction and does not depend on the image resolution. On the other hand, the transformation given in (6) must be an increasing function in the interval $[0, r_{max}]$ (otherwise the lens distortion model is not well defined). In particular, its derivative must be positive, which leads to the following conclusion:

$$1 + 3k_1 r^2 > 0 \quad \forall r \in [0, r_{max}] \;\Rightarrow\; k_1 > -\frac{1}{3r_{max}^2}. \tag{9}$$

We observe that, in terms of p, the above condition leads to

$$p > -1/3. \tag{10}$$

The distribution of the votes for a given value of the distortion parameter is illustrated in Fig. 1. If no distortion is considered (see Fig. 1(a)), the votes are not so clearly concentrated, since the points do not fit into the line equations in a satisfactory way and different segments of the same line vote for different equations in the Hough space. On the other hand, when distortion is included (see Fig. 1(b)), there is a matching between the points and the equations, so that the location of the maximum in the Hough space is more clearly determined.

4. Lens distortion correction

An interesting use of the proposed automatic line detection method is to apply it to correct the distortion in images showing a significant radial distortion caused by the lens. By using the technique presented above, the lines within the image are detected. Note that, although the method we propose will work for the case of detecting only one line, the total RMS error (sum of the squares of the distances from the undistorted points to the lines for all the detected lines) is strongly reduced when dealing with more lines. For the set of detected lines we apply the two-parameter model, which has shown excellent performances when correcting the radial distortion from a single image (Alvarez et al., 2008). Additionally, we will assume that the center of distortion is the center of the image.

Figure 2 illustrates the stages in the process to correct the distortion. First, the edges are extracted using a subpixel edge detection algorithm. Second, the improved Hough transform is used to extract the lines by considering the distortion parameter in the Hough space. This provides an initial approximation for the model. Finally, the two-parameter distortion model is optimized and applied to correct the distortion.

To obtain the distortion-free image I, it is necessary to calculate the corresponding pixel position in the distorted image I' for each pixel of I. Then, by means of biquadratic interpolation, the pixel intensity is determined and I can suitably be rebuilt. To perform this mapping, it is necessary to invert the radial distortion model. Therefore, we look for a radial function $G(\hat{r})$ such that

$$\begin{pmatrix} x - x_c \\ y - y_c \end{pmatrix} = G(\hat{r}) \begin{pmatrix} \hat{x} - x_c \\ \hat{y} - y_c \end{pmatrix}, \tag{11}$$

where

$$\hat{r} = \sqrt{(\hat{x} - x_c)^2 + (\hat{y} - y_c)^2}. \tag{12}$$

From the above expression, we obtain that

$$r = G(\hat{r})\hat{r}. \tag{13}$$

On the other hand, we have that

$$\begin{pmatrix} \hat{x} - x_c \\ \hat{y} - y_c \end{pmatrix} = L(r) \begin{pmatrix} x - x_c \\ y - y_c \end{pmatrix}, \tag{14}$$

and, therefore,

$$\hat{r} = L\left(G(\hat{r})\hat{r}\right) G(\hat{r})\hat{r}. \tag{15}$$

So we conclude that $G(\hat{r})$ is a root of the polynomial

$$P(\lambda) = 1 - L(\lambda\hat{r})\lambda = 1 - \sum_{j=0}^{N_k} k_j \hat{r}^j \lambda^{j+1}. \tag{16}$$

In order to minimize the distance between the distorted and undistorted points, we choose, among all possible real roots of $P(\lambda)$, the one nearest to 1.

5. Experimental results

In order to test our technique, we have applied it to some images showing a significant distortion. A range of possible distortion values are tested with the aim of finding the value which makes the points fit best in the line equations.

Our Hough space is a three-dimensional discrete space in which the distortion parameter, the orientation and the distance to the origin are discretized within their respective ranges, i.e. $[-1/3, 1]$ for the percentage of correction p (the lower bound is given by the condition (10) and the upper bound was fixed in order to allow up to a 100% of distortion correction radial variation), $[0, \pi]$ for the orientation, and $[-d, d]$ for the distance to the origin (where $d = \sqrt{(image\ width)^2 + (image\ height)^2}$).

Figures 3, 4, 5 and 6 illustrate the application of the line detection process to the correction of the distortion in some images. From the gray-level image, the edges are extracted. They are used in the voting procedure to identify the lines (we use different colors to distinguish the lines which have been recognized) and determine the most likely value for the distortion parameter. From this distortion parameter, the two-parameter model is estimated and the image is corrected, as explained in section 4. Figure 3 (2731×1822 pixels) contains a calibration pattern in which 24 lines are visible. As observed in Fig. 3(c), when distortion is not taken into account, the lines which are far away from the center (and therefore more affected by the distortion) are not completely identified. In addition, some segments which should match the same line equation are considered as parts of different lines (see, for instance, the upper sides of the squares in the second row, which appear in different colors, since they have not been associated). However, when distortion is considered, all the segments of the 24 lines match their equations and are perfectly recognized (see Fig. 3(d)). Since these lines are the basis for correcting the distortion, and the longer the lines, the more useful the information they provide, when the distortion parameter is not considered in the Hough transform, the distortion is only slightly corrected (see Fig. 3(e)). Nevertheless, when the lines have been identified using the Hough transform which includes the distortion parameter, the resulting distortion-free image is much more satisfactory (see Fig. 3(f)). Since the correction modifies the size of the resulting images, they have been scaled to the size of the original images for presentation purposes.

In Fig. 4 (2707×1800 pixels) and Fig.5 (2881×1909 pixels), when the distortion parameter is not considered, many lines are not detected (e.g. left side of the frame or top of the building). However, the inclusion of the distortion parameter in the Hough space allows us to detect more lines, and the longest ones are not split (different segments which appear in a different color when this parameter is not taken into account, are now associated to the same line). As observed in Fig. 4(f) and Fig. 5(f), the frame and the building are almost perfectly lined-up after the distortion has been corrected.

Figure 6 (2560×1920 pixels) is special, since this case presents a considerable pincushion type distortion. Although some lines are detected without including the distortion parameter, the upper and lower horizontal lines, which are strongly affected by the pincushion distortion, are only detected when the distortion parameter is considered. For that reason, the result in Fig. 6(f) shows an almost perfectly lined-up door.

Figures 7 (1024×680 pixels)[1] and 8(1024×510 pixels) [2] have been ob-

[1] "Usno" by US Air Force CC0 http://commons.wikimedia.org/wiki/File:Usno-amc.jpg

[2] "Church Street" by Gryffindor CC0 http://commons.wikimedia.org/wiki/File:90_Church_Street_fisheye.jpg

tained from a publicly available database. They are both characterized by a strong fihseye distortion which bends the straight lines very much and makes them extremely difficult to extract. As observed, long straight lines are split into different segments when the distortion parameter is not included. However, using the improved Hough transform which includes the distortion parameter allows identifying long lines (see Fig. 7(d) and 8(d)) and correcting the distortion in a quite satisfactory way (see Fig. 7(f) and 8(f)).

In these experiments, instead of finding *ad hoc* values for each situation, we have used the same set of parameters for all of them. For instance, using figure 3(a) as a reference, we have set the number of lines to be selected for every value of the distortion parameter to 24, which is the number of lines in the calibration pattern.

Figure 9 illustrates how the maximum number of votes varies within the Hough space according to the distortion parameter. In these examples we can see that, when we approach the actual value of the parameter, the maximum increases, due to the fact that the edge points fit in the line equations. As observed, the calibration pattern in Fig. 3 and the painting in Fig. 4 present a clear peak in the maximum value. For the building in Fig. 5, the peak is softer, since the quality of the available information is lower. As expected, for the door in Fig. 6, which has pincushion distortion, the value of the distortion parameter for which the maximum is reached is negative. For the images in Fig. 7 and Fig. 8, which present fisheye distortion, the magnitude of p is much higher.

Table 1 shows some quantitative results which illustrate how the introduc-

Image	Number of points ND	Number of points	Correction ND	Correction
Pattern	11984	19277	-0.27%	9.40%
Painting	11845	17881	0.92%	8.24%
Building	9524	11921	0.20%	10.75%
Door	11965	14350	-1.63%	-9.52%
Usno	1572	2585	8.19%	45.38%
Church street	1727	1974	0.09%	59.76%

Table 1: Comparison of the number of points detected and the percentage of correction between the models with and without the distortion parameter (ND stands for No Distortion, i.e. when the distortion parameter is not taken into account).

tion of the distortion parameter in the Hough space provides a more accurate detection of the lines and a better correction of the distortion. Firstly, we have considered the number of points in the lines which have been detected. As observed, it is considerably higher in all images when the Hough space includes the distortion parameter. Secondly, we have compared the percentage of correction introduced in Eq.(7). When the distortion parameter is not included, the magnitude of the correction is extremely low and even the sign may be wrong (see, for instance, the pattern). This does not allow obtaining satisfactory undistorted images. However, when the Hough space with distortion parameter is used, both the sign and the magnitude of the correction are coherent with the distortion of the images, which results in quite satisfactory undistorted images (as expected, it is negative for the case of pincushion distortion, as in Fig. 6).

6. Conclusions

In this paper we have presented a new approach to detect lines in images showing a significant lens radial distortion. The technique introduced is automatic and is mainly intended for images containing the projection of visible 3D lines. The identification of the lines is performed by means of a new Hough transform which includes the radial distortion as a parameter. Using a three-dimensional Hough space, we are able to detect the lines and estimate the distortion parameter. Once the lines have been detected, an algebraic lens distortion model with two distortion parameters is applied to estimate and correct the lens distortion. Therefore, this method automatically recognizes the distorted lines and provides a distortion-free image, more suitable for a postprocessing analysis. We have presented a variety of experiments on real images where we show that the proposed method allows to remove effectively the lens distortion and outperforms the results obtained using the standard Hough transform.

Acknowledgement

This research has partially been supported by the MICINN project reference MTM2010-17615 (Ministerio de Ciencia e Innovación. Spain).

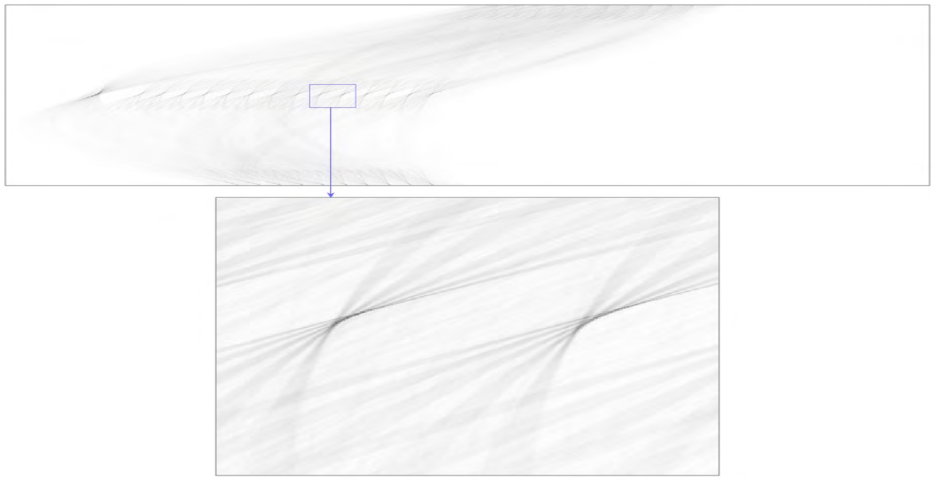

(a)

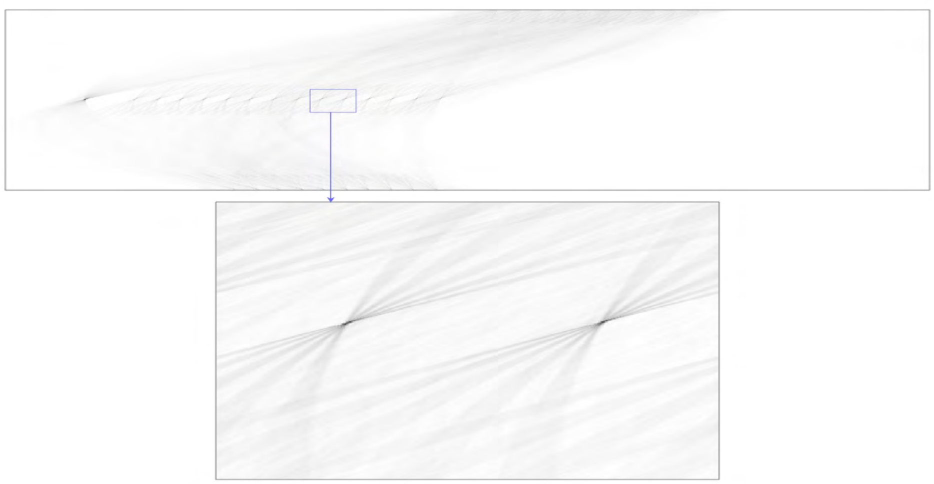

(b)

Figure 1: General view and zoom of the distribution of the votes within the Hough space for the pattern in figure 3: (a) without considering the distortion parameter; (b) using the distortion value for which the maximum is reached. The horizontal direction represents the distance to the origin and the vertical direction represents the orientation of the lines.

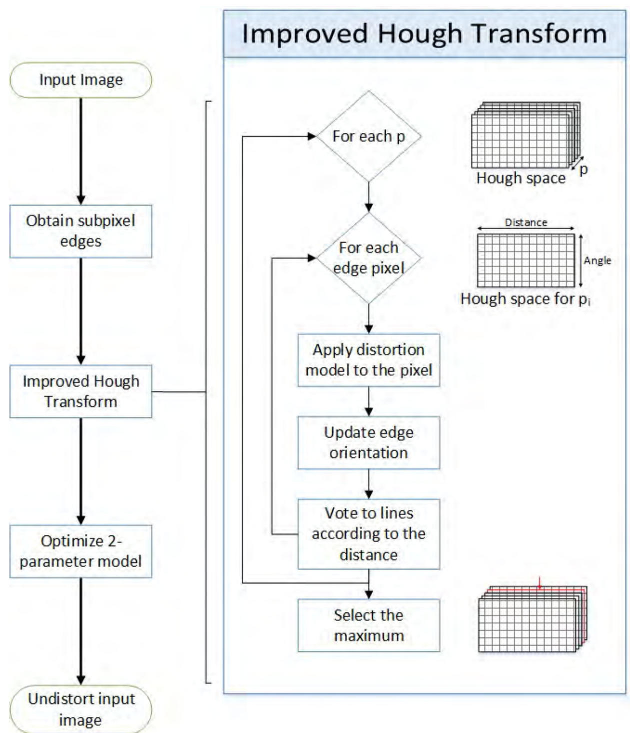

Figure 2: Flowchart for the correction of the distortion, including the stage corresponding to the improved Hough transform.

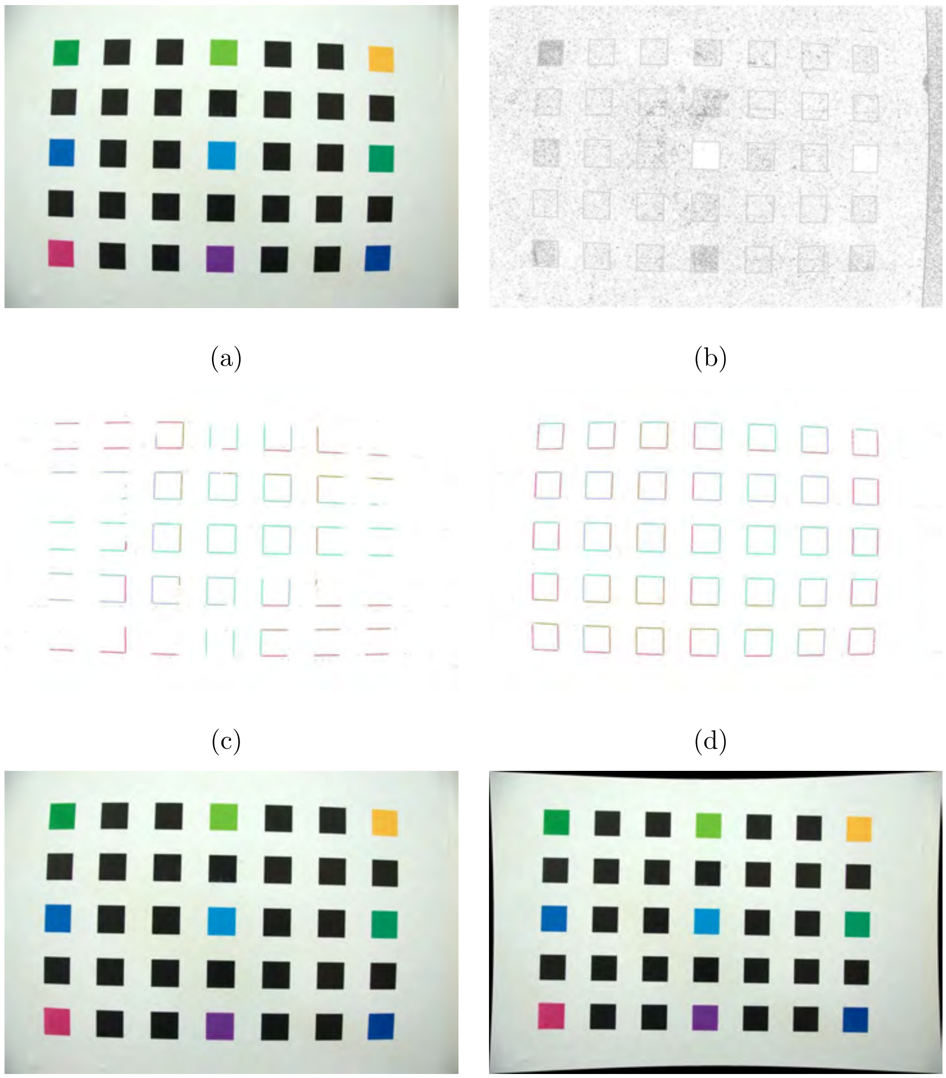

Figure 3: Lens distortion correction: (a) Original image, (b) edges extracted from the image, (c) lines using the Hough transform without considering the distortion parameter, (d) lines using the improved Hough transform considering the distortion parameter, (e) undistorted image from the 2 parameter model using lines in (c), and (f) undistorted image from the 2 parameter model using lines in (d) ($k_1 = 4.51 \times 10^{-3}$; $k_2 = -3.79 \times 10^{-11}$).

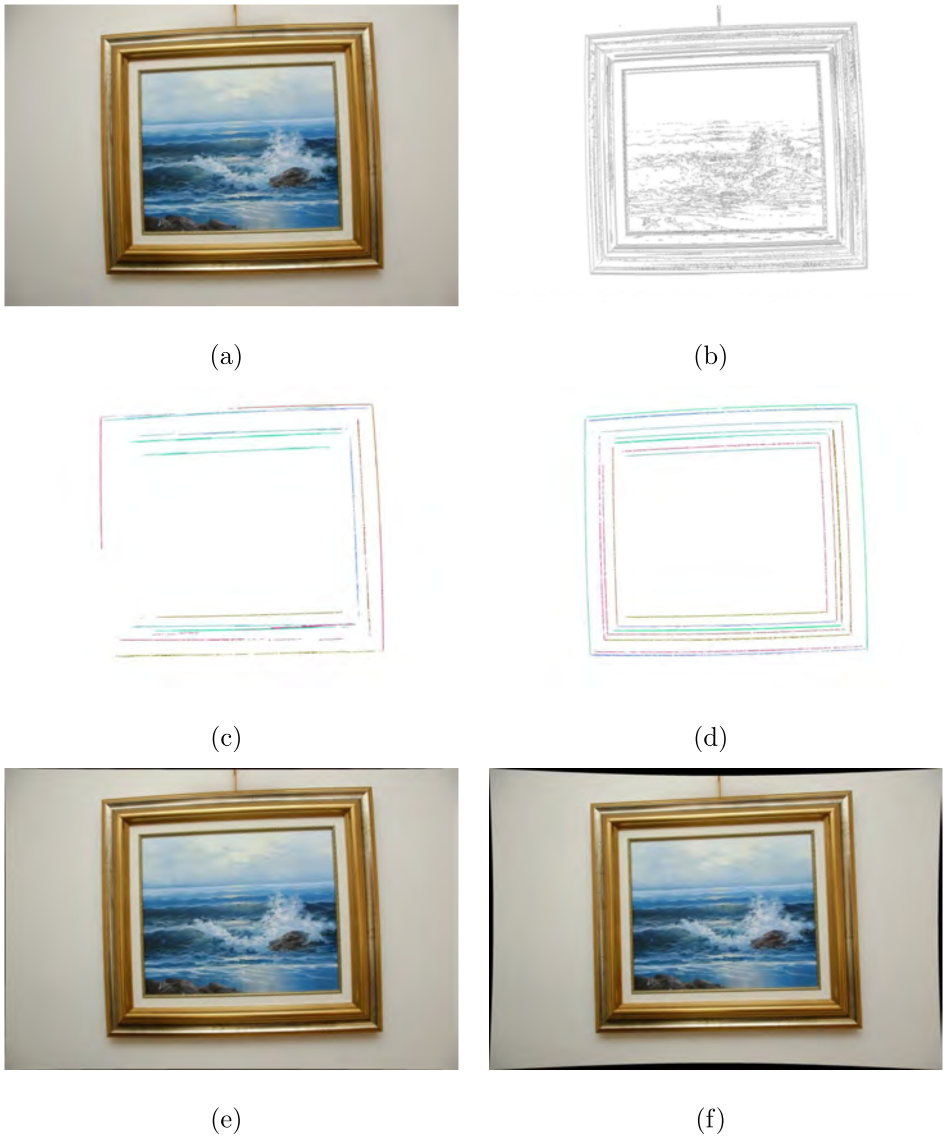

Figure 4: Lens distortion correction: (a) Original image, (b) edges extracted from the image, (c) lines using the Hough transform without considering the distortion parameter, (d) lines using the improved Hough transform considering the distortion parameter, (e) undistorted image from the 2 parameter model using lines in (c), and (f) undistorted image from the 2 parameter model using lines in (d) ($k_1 = 3.90 \times 10^{-3}$; $k_2 = -2.97 \times 10^{-15}$).

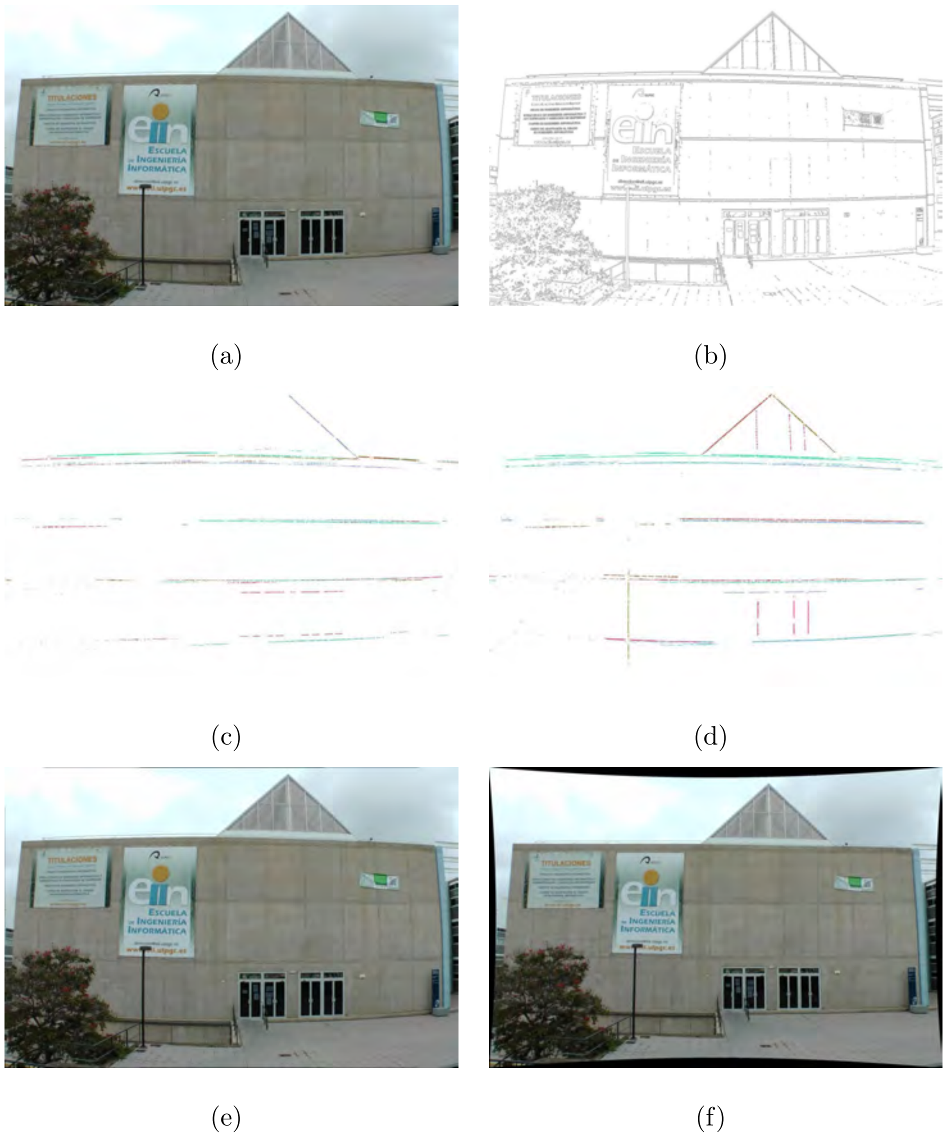

Figure 5: Lens distortion correction: (a) Original image, (b) edges extracted from the image, (c) lines using the Hough transform without considering the distortion parameter, (d) lines using the improved Hough transform considering the distortion parameter, (e) undistorted image from the 2 parameter model using lines in (c), and (f) undistorted image from the 2 parameter model using lines in (d) ($k_1 = 3.36 \times 10^{-3}$; $k_2 = 8.09 \times 10^{-11}$).

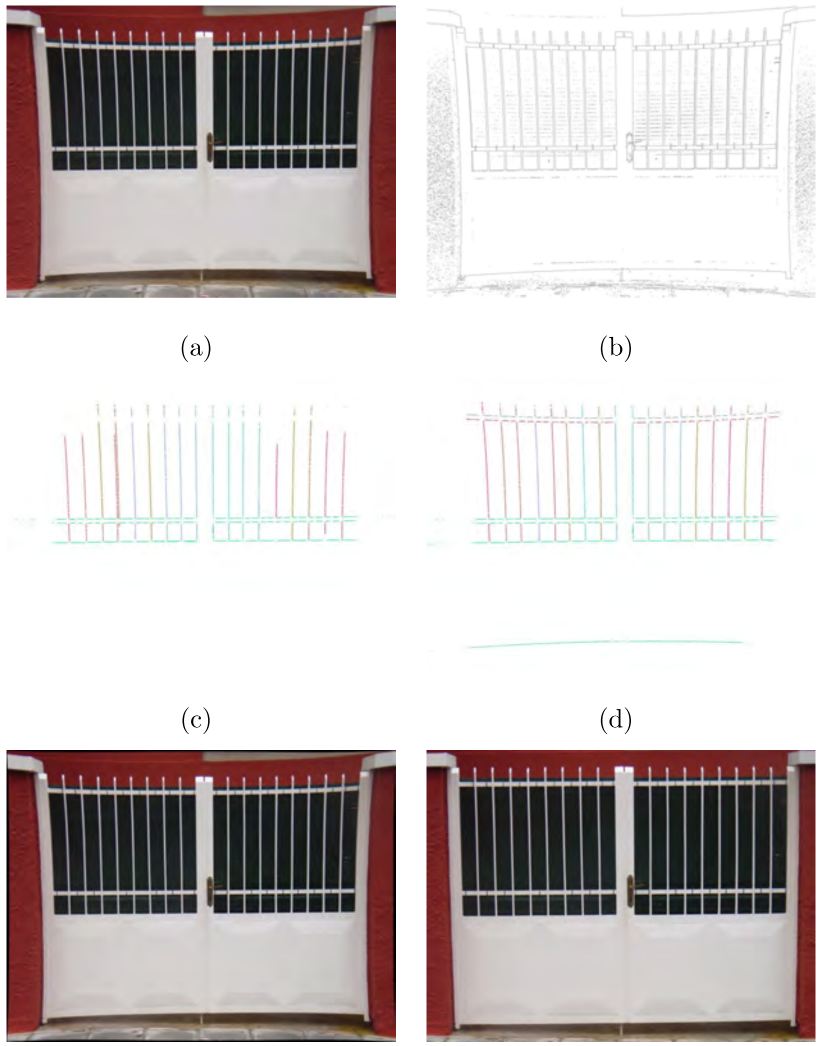

(a) (b) (c) (d) (e) (f)

Figure 6: Lens distortion correction: (a) Original image, (b) edges extracted from the image, (c) lines using the Hough transform without considering the distortion parameter, (d) lines using the improved Hough transform considering the distortion parameter, (e) undistorted image from lines obtained without considering the distortion parameter, and (f) undistorted image from lines obtained considering the distortion parameter ($k_1 = -3.77 \times 10^{-8}$; $k_2 = 1.86 \times 10^{-11}$).

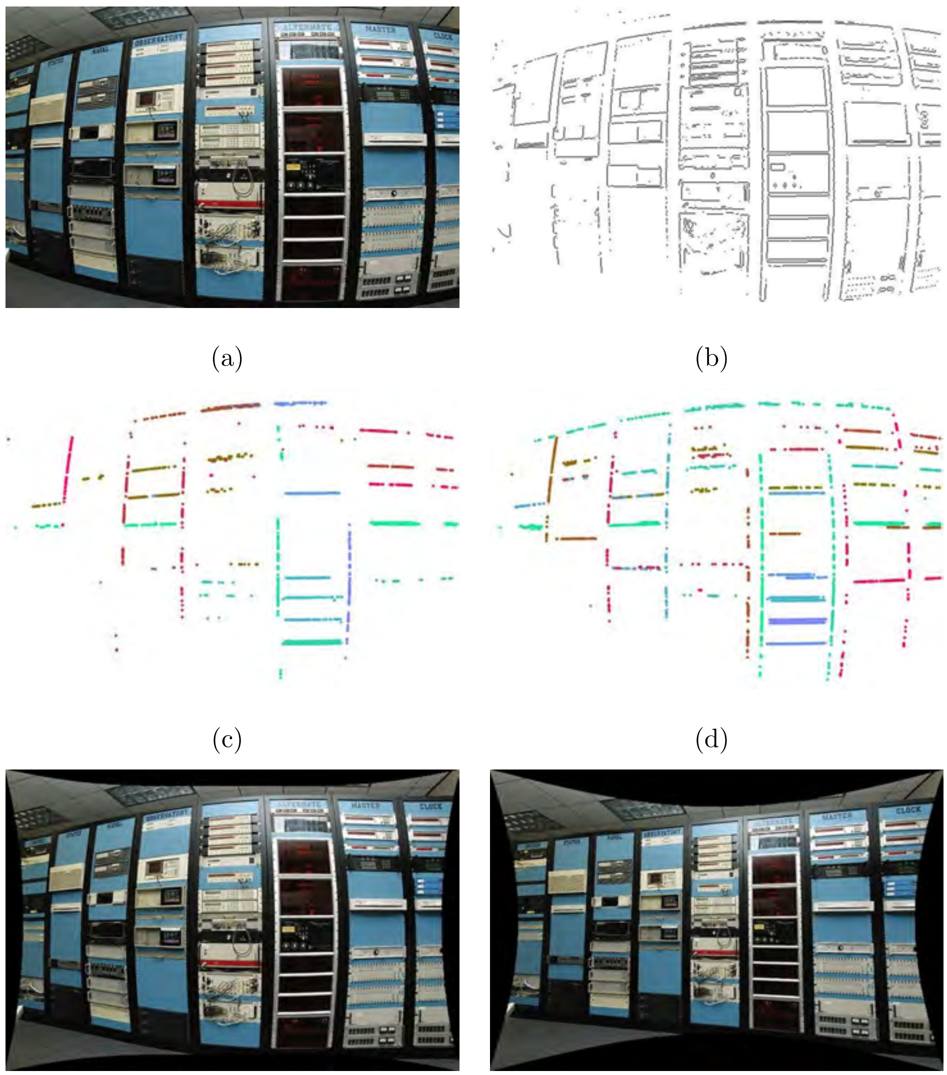

(a) (b)

(c) (d)

(e) (f)

Figure 7: Lens distortion correction: (a) Original image, (b) edges extracted from the image, (c) lines using the Hough transform without considering the distortion parameter, (d) lines using the improved Hough transform considering the distortion parameter, (e) undistorted image from lines obtained without considering the distortion parameter, and (f) undistorted image from lines obtained considering the distortion parameter ($k_1 = 1.57 \times 10^{-1}$; $k_2 = 1.02 \times 10^{-6}$).

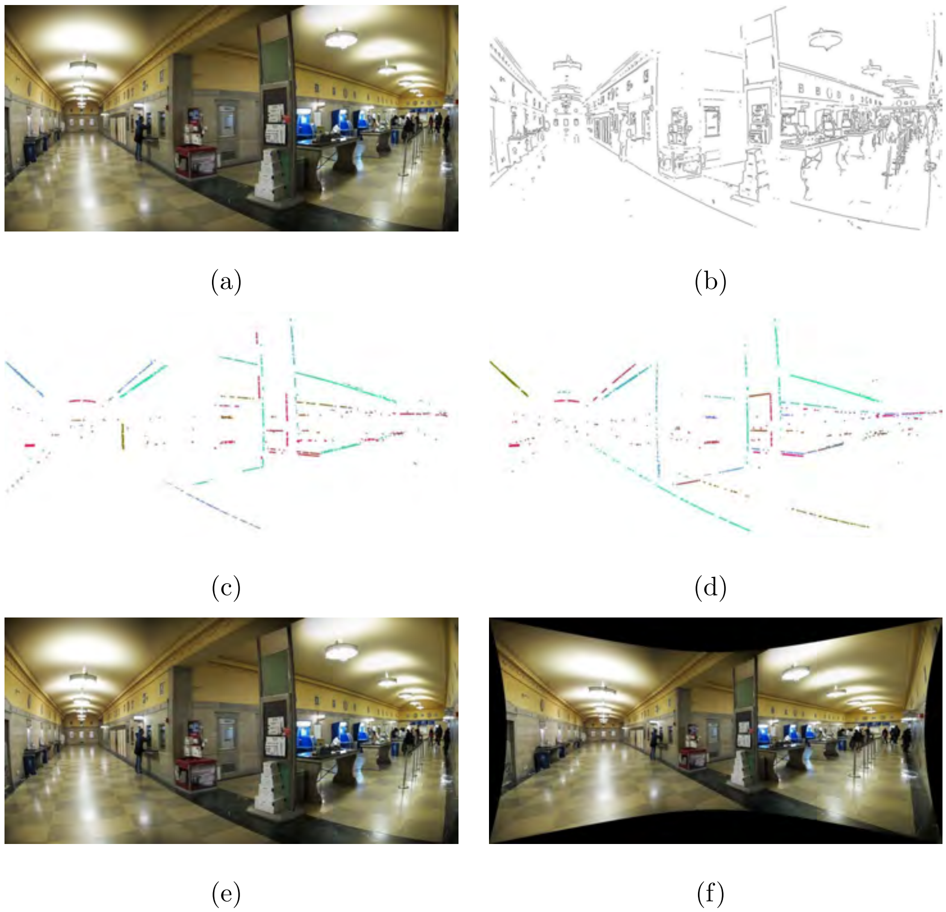

Figure 8: Lens distortion correction: (a) Original image, (b) edges extracted from the image, (c) lines using the Hough transform without considering the distortion parameter, (d) lines using the improved Hough transform considering the distortion parameter, (e) undistorted image from lines obtained without considering the distortion parameter, and (f) undistorted image from lines obtained considering the distortion parameter ($k_1 = 1.06 \times 10^{-1}$; $k_2 = 2.16 \times 10^{-8}$).

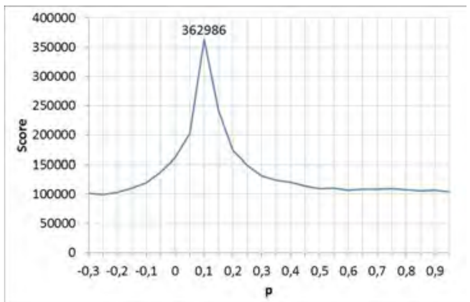

(a) Pattern

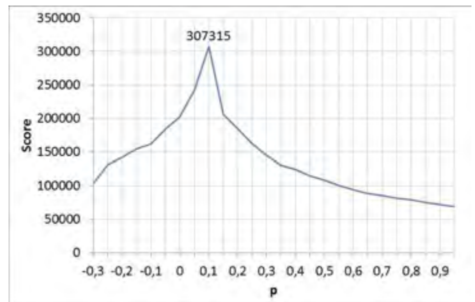

(b) Painting

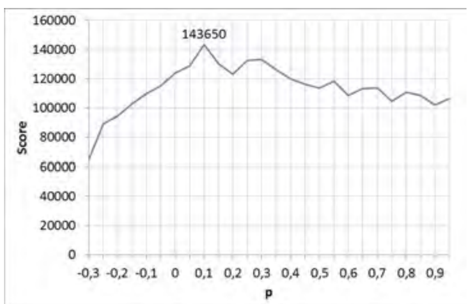

(c) Building

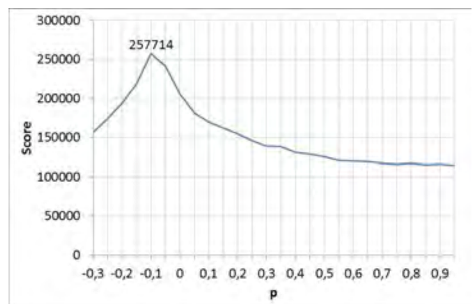

(d) Door

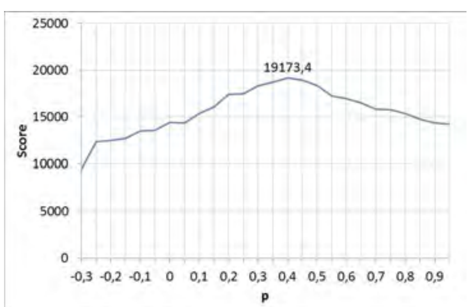

(e) Usno

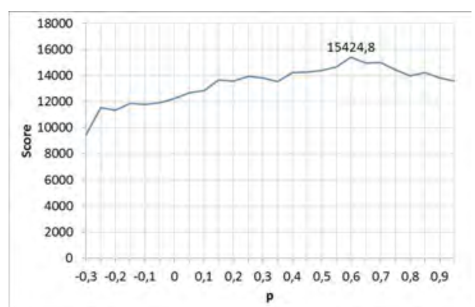

(f) Church_street

Figure 9: Values of the maximum in the voting matrix with respect to the percentage of distortion correction.

References

Alvarez, L., Gomez, L., Henriquez, P., 2012. Zoom dependent lens distortion mathematical models. Journal of Mathematical Imaging and Vision 44, 480–490.

Alvarez, L., Gomez, L., Sendra, R., 2008. An algebraic approach to lens distortion by line rectification. Journal of Mathematical Imaging and Vision 39, 36–50.

Alvarez, L., Gomez, L., Sendra, R., 2010. Algebraic lens distortion model estimation. Image Processing On Line. http://www.ipol.im .

Alvarez, L., Gomez, L., Sendra, R., 2011. Accurate depth dependent lens distortion models: an application to planar view scenarios. Journal of Mathematical Imaging and Vision 39, 75–85.

Ballard, D.H., 1981. Generalizing the Hough transform to detect arbitrary shapes. Pattern Recognition 13, 111–122.

Barnard, S., 1983. Interpreting perspective images. Artif. Intell. 21, 435–462.

Bräuer-Burchardt, C., Heinze, M., Munkelt, C., Kühmstedt, P., Notni, G., 2006. Distance dependent lens distortion variation in 3d measuring systems using fringe projection. In: Proc. BMVC , 327–336.

Brown, D., 1971. Close-range camera calibration. Photogrammetric Engineering 37, 855–866.

Bukhari, F., Dailey, M., 2010. Robust radial distortion from a single image. Lecture Notes in Computer Science 6454, 11–20.

Bukhari, F., Dailey, M., 2012. Automatic radial distortion estimation from a single image. Journal of Mathematical Imaging and Vision 45, 31–45.

Chung, K.L., Lin, Z.W., 2010. New orientation-based elimination approach for accurate line-detection. Pattern Recognition Letters 31, 11–19.

Devernay, F., Faugeras, O., 2001. Straight lines have to be straight. Machine Vision and Applications 13, 14–24.

Duda, R.O., Hart, P.E., 1972. Use of the hough transformation to detect lines and curves in pictures. Commun. ACM 15, 11–15.

Faugeras, O., 1993. Three-dimensional computer vision. MIT Press.

Faugeras, O., Luong, Q., Maybank, S., 1992. Camera self-calibration: Theory and experiments. Lecture Notes in Computer Science 588, 321–334.

Faugeras, O., Luong, Q., Papadopoulo, T., 2001. The geometry of multiple image. MIT Press.

Faugeras, O., Toscani, G., 1987. Structure from motion using the reconstruction and reprojection technique. In: Proc. IEEE Workshop on Computer Vision (IEEE Computer Society) , 345–348.

Fitzgibbon, A.W., 2001. Simultaneous linear estimation of multiple view geometry and lens distortion. In: Proc. IEEE International Conference on Computer Vision and Pattern Recognition , 125–132.

Fraser, C., Shortis, M., 1992. Variation of distortion within the photographic field. Photogramm. Eng. Remote Sensing 58, 851–855.

Gonzalez-Aguilera, D., Gomez-Lahoz, J., Rodriguez-Gonzalvez, P., 2011. An automatic approach for radial lens distortion correction from a single image. IEEE Sensors Journal 11 11, 956–965.

Guru, D.S., Shekar, B.H., Nagabhushan, P., 2004. A simple and robust line detection algorithm based on small eigenvalue analysis. Pattern Recognition Letters 25, 1–13.

Hartley, R.I., Zisserman, A., 2004. Multiple view geometry in computer vision. Cambridge University Press.

Hough, P.V.C., 1959. Machine Analysis of Bubble Chamber Pictures, in: International Conference on High Energy Accelerators and Instrumentation, CERN.

Kang, S., 2000. Radial distortion snakes. In: Proc. IEICE Transactions on Information and Systems , 1603–1611.

Lee, Y.S., Koo, H.S., Jeong, C.S., 2006. A straight line detection using principal component analysis. Pattern Recognition Letters 27, 1744–1754.

McGlone, C., 1980. Manual of Photogrammetry. Amer. Soc. of Photogrammetry. 4th edition.

Ramalingam, S., Sturm, P., Lodha, S., 2010. Generic self-calibration of central cameras. Computer Vision and Image Understanding 114, 210–219.

Strand, R., Hayman, E., 2005. Correcting radial distortion by circle fitting. In: Proc. British Machine Vision Conference, (BMVC) .

Tsai, R., 1987. A versatile camera calibration technique for high-accuracy 3d machine vision metrology using off-the-shelf tv cameras and lenses. IEEE Journal of Robotics and Automation 3, 323–344.

Wang, A., Qiu, T., Shao, L., 2009. A simple method to radial distortion correction with centre of distortion estimation. Journal of Mathematical Imaging and Vision 35, 165–172.

Zhang, Z., 2000. A flexible new technique for camera calibration. IEEE Transactions on Pattern Analysis and Machine Intelligence 22, 1330–1334.